JOURNAL OF BACTERIOLOGY, Dec. 1992, p. 7716–7728
0021-9193/92/237717-12$02.00/0

Vol. 174, No. 23

FtsL, an Essential Cytoplasmic Membrane Protein Involved in Cell Division in *Escherichia coli*

LUZ-MARIA GUZMAN,[1] JAMES J. BARONDESS,[1,2] AND JON BECKWITH[1]*

Department of Microbiology and Molecular Genetics[1] and Program in Cell and Developmental Biology,[2] Harvard Medical School, 200 Longwood Avenue, Boston, Massachusetts 02115

Received 25 June 1992/Accepted 9 September 1992

We have identified a gene involved in bacterial cell division, located immediately upstream of the *ftsI* gene in the min 2 region of the *Escherichia coli* chromosome. This gene, which we named *ftsL*, was detected through characterization of Tn*phoA* insertions in a plasmid containing this chromosomal region. Tn*phoA* topological analysis and fractionation of alkaline phosphatase fusion proteins indicated that the *ftsL* gene product is a 13.6-kDa cytoplasmic membrane protein with a cytoplasmic amino terminus, a single membrane-spanning segment, and a periplasmic carboxy terminus. The *ftsL* gene is essential for cell growth and division. A null mutation in *ftsL* resulted in inhibition of cell division, formation of long, nonseptate filaments, ultimate cessation of growth, and lysis. Under certain growth conditions, depletion of FtsL or expression of the largest *ftsL-phoA* fusion produced a variety of cell morphologies, including Y-shaped bacteria, indicating a possible general weakening of the cell wall. The FtsL protein is estimated to be present at about 20 to 40 copies per cell. The periplasmic domain of the protein displays a sequence with features characteristic of leucine zippers, which are involved in protein dimerization.

In *Escherichia coli*, cell division is characterized by the formation of a septum at the middle of the elongating rod-shaped cell. This process requires the precise regulation of cell envelope growth and orientation in concert with other processes which take place in the cytoplasm (reviewed in references 9 and 11). Genetic studies have identified several genes involved in septum formation based on the characterization of temperature-sensitive mutants that form nonseptate filaments at the nonpermissive temperature (*fts* genes) (14). Many of these genes are clustered in the min 2 region of the chromosome, which also contains a number of genes involved in cell envelope biosynthesis (11, 25). This interval of about 17 kb, from the 5′-proximal gene (*ftsI*) to the distal ones (*ftsQ*, *ftsA*, *ftsZ*, and *envA*), comprises some 15 genes arranged in the same orientation, very close to each other, and in several cases overlapping (19, 25, 27, 31). The region has numerous promoters and a complex pattern of transcriptional and translational regulation (26, 31, 41).

Some of the best-characterized cell division genes map to this min 2 region. For instance, the *ftsZ* gene has been implicated in the regulation of septum initiation and is the target of several endogenous cell division inhibition systems (17, 19). Recent studies have also indicated that FtsZ is assembled into a ring structure at the septum (4) and that it could be involved in coupling nucleoid separation and septation (37). Penicillin-binding protein PBP3 (35), the product of the *ftsI* gene, is a membrane protein specifically required during septation (16, 34) and appears to have enzymatic functions for the polymerization and cross-linking of glycan subunits in the cell wall (16).

Despite these examples of well-defined cell division proteins, it is notable that the functions of most *E. coli* cell division genes, whether located in the min 2 cluster or in other chromosomal regions, are largely unknown. Even genes like *ftsQ* (8) and *ftsA* (38), whose essentiality for cell division has been well established, do not have a precise known function.

A useful step towards defining the function of cell division proteins is to establish their subcellular localization. The cytoplasmic membrane must play a major role in the processes that regulate envelope rearrangements during the cell cycle, for instance, in signal transduction pathways or septum initiation and formation. Thus, cell division proteins localized to this compartment are likely to be involved in these processes and to play a key role in cell division. In this communication, we report the identification and initial characterization of another min 2 gene involved in cell division whose product is an essential cytoplasmic membrane protein.

MATERIALS AND METHODS

Chemical reagents. 5-Bromo-5-chloro-3-indolylphosphate (XP) was obtained from Bachem Fine Chemicals (Torrance, Calif.) and used at 40 μg/ml on plates. L-Arabinose was obtained from Pfanstiehl Laboratories Inc. (Waukegan, Ill.). Restriction enzymes, T4 DNA ligase, and Vent Polymerase were purchased from New England BioLabs, Inc. (Beverly, Mass.), and L-[^{35}S]methionine (1,000 Ci/mmol) was obtained from Amersham Corporation (Arlington Heights, Ill.).

Bacterial strains and media. Bacterial strains are listed in Table 1. The *degP* allele from strain KS474 [KS272 *degP41* (Δ*Pst*I-Kan^r) (36)] was introduced into DHB4 by P1 transduction (24), selecting for Kan^r. The *recA*-deficient strains were constructed by P1 transduction of a *recA*::*cat* allele from strain BW10724 (a gift of Barry Wanner), selecting with 10 μg of chloramphenicol per ml. The *fts*(Ts) allele of strain JJ143 was obtained from strain TOE-23 (3) by P1 transduction.

Rich media were NZY liquid broth and agar, which differ from LB (24) in that tryptone is replaced by NZ amine and the salt concentration is 8 g of NaCl per liter. Defined minimal medium was M63 (24) with 18 amino acids (no methionine or cysteine), thiamine (1 μg/ml), and 0.2% of the

* Corresponding author.

TABLE 1. *E. coli* strains

Strain	Genotype	Source or reference
DHB4	*araD139* Δ(*ara-leu*)*7697* Δ*lacX74 galE galK rpsL* Δ*malF3* Δ*phoA* (*Pvu*II) *thi phoR*/F'*lacI*^{q} *pro lac*	7
KS272	F$^-$ Δ*lacX74 galE galK thi rpsL* Δ*phoA* (*Pvu*II)	36
MPh42	F$^-$ *araD139* Δ(*ara-leu*)*7697* Δ*lacX74 galE galK rpsL phoR*	Laboratory collection
MC4100	F$^-$ *araD139 lac*Δ*U169 relA1 rpsL150 thi mot flbB5301 deoC7 ptsF25 rbsR*	Laboratory collection
JJ143	MC4100 *ftsI*(Ts) *recA*	This study
MJC98	KS272 *pcnB-80 zid1*::Tn*10*	Michael Carson[a]
MJC122	KS272 *leu*::Tn*10*	8
MJC224	KS272 *polA*(Ts-12) *zig*::Tn*10*	8
MJC251	MJC122 *ftsQ*::Tn*phoA187* (λ16-25)	8
MJC252	MJC122 *ftsQ*::Tn*phoA80* (λ16-25)	8
LMG72	DHB4/pZ26::Tn*phoA*L81ΔIS*50*R	This study
LMG83	MJC122 *ftsL*::Tn*phoA*L81ΔIS*50*R/pZ26	This study
LMG89	MJC98 *ftsL*::Tn*phoA*L81Δ1S*50*R/pLMG180	This study
LMG97	MJC122/pZ26	This study
LMG142	DHB4 *ftsL*::Tn*phoA*L81ΔIS*50*R/pLMG180	This study
LMG145	MJC122 *ftsL*::Tn*phoA*L81ΔIS*50*R/pLMG180	This study
LMG148	MJC122/pLMG180	This study
LMG149	MJC122/pBAD18	This study
LMG170	DHB4 *degP41*	This study
LMG171	LMG170/pZ26	This study
LMG172	LMG170/pZ26::Tn*phoA*L81	This study
LMG173	LMG170/pZ26::Tn*phoA*L88	This study
LMG174	LMG170/pZ26::Tn*phoA*L112	This study
LMG175	LMG170/pZQ::Tn*phoA*A80	This study
LMG177	MJC122/pLMG182	This study

[a] State University of New York College at Cortland.

specified carbon source. Antibiotics were used at the following concentrations: ampicillin, 200 μg/ml (unless otherwise indicated); kanamycin, 40 μg/ml; tetracycline, 20 μg/ml.

Antibodies. Polyclonal anti-alkaline phosphatase (anti-AP) antibody was made by C. Gardel in this laboratory. Anti-glucose 6-phosphate dehydrogenase and anti-MalF were kindly supplied by the D. Fraenkel Laboratory and B. Traxler (this laboratory), respectively. Anti-β-lactamase was purchased from 5 prime-3 prime, Inc. (Boulder, Colo.), and anti-OmpA was kindly provided by C. Kumamoto.

Plasmid constructs and DNA sequencing. Plasmids are described in Fig. 1. DNA sequence analysis was performed using double-stranded plasmid miniprep DNA (8a) and Sequenase (U.S. Biochemical, Cleveland, Ohio) as recommended by the manufacturer. DNA from DH5α strains (Bethesda Research Laboratories, Inc., Gaithersburg, Md.) containing the different pZ26::Tn*phoA* plasmids was sequenced using primers complementary to the 5′ and 3′ ends of the Tn*phoA* transposon (7). Compressions were resolved by running dGTP and dITP reactions on 7 M urea–25% formamide gels.

Isolation of AP fusions and AP assays. Tn*phoA* insertions in plasmid pZ26 were isolated using λTn*phoA* as previously described (20). AP activity was measured by determining the rate of *p*-nitrophenyl phosphate hydrolysis as previously described (23), using permeabilized cells incubated at 28°C.

Cell fractionation and detection of AP fusions. Logarithmic-phase cultures of strains growing in glycerol-minimal medium (5 ml) were pulse-labeled with 100 μCi of [^{35}S]methionine per ml for 2 min. Cultures were then transformed into spheroplasts and centrifuged to separate the supernatant (periplasm) and pellet (spheroplasts) fractions as previously described (13). Spheroplasts were lysed by rapid resuspension in ice-cold water and subsequently centrifuged at high speed to obtain the envelope and cytoplasmic fractions (13). The envelope fraction was then further fractionated into cytoplasmic and outer membranes by differential solubilization with Sarkosyl (13). Samples corresponding to equivalent amounts of cells from each fraction were immunoprecipitated with antibodies against AP and analyzed by polyacrylamide gel electrophoresis (PAGE) as previously described (36). Immunoprecipitated protein markers for the intracellular (glucose 6-phosphate dehydrogenase), inner membrane (MalF), periplasmic (β-lactamase), and outer membrane (OmpA) fractions were found in the appropriate compartments.

Specific activity of FtsL-AP fusion proteins. Determination of the specific activity of FtsL-AP fusion proteins relative to wild-type AP was performed as previously described (8), with several differences. *degP* mutant strains (36) were used to increase the stability of the FtsL-AP fusions, which otherwise were significantly degraded during a 15-min pulse-labeling and chase in a *degP*$^+$ background. The amount of OmpA present in the samples in which AP was to be quantified was used as an internal control. Incorporated [^{35}S]methionine was measured by exposing dried gels to a phosphor screen and scanning the screen on a phosphorimager (series 400; Molecular Dynamics). The resulting data were analyzed by using ImageQuant software (version 3.0). Synthesis rates were calculated by dividing the amount of fusion protein or wild-type AP by the amount of OmpA during the pulse, after correction for the number of methionine residues in each of the FtsL-AP fusions and in wild-type AP. The specific activity was then defined as follows: FtsL-AP enzymatic activity relative to wild-type AP/FtsL-AP protein synthesis rate relative to wild-type AP.

Construction of the *ftsL* null mutation. The Tn*phoA* transposon insertion L81 on plasmid pZ26 (pZ26::Tn*phoA*L81)

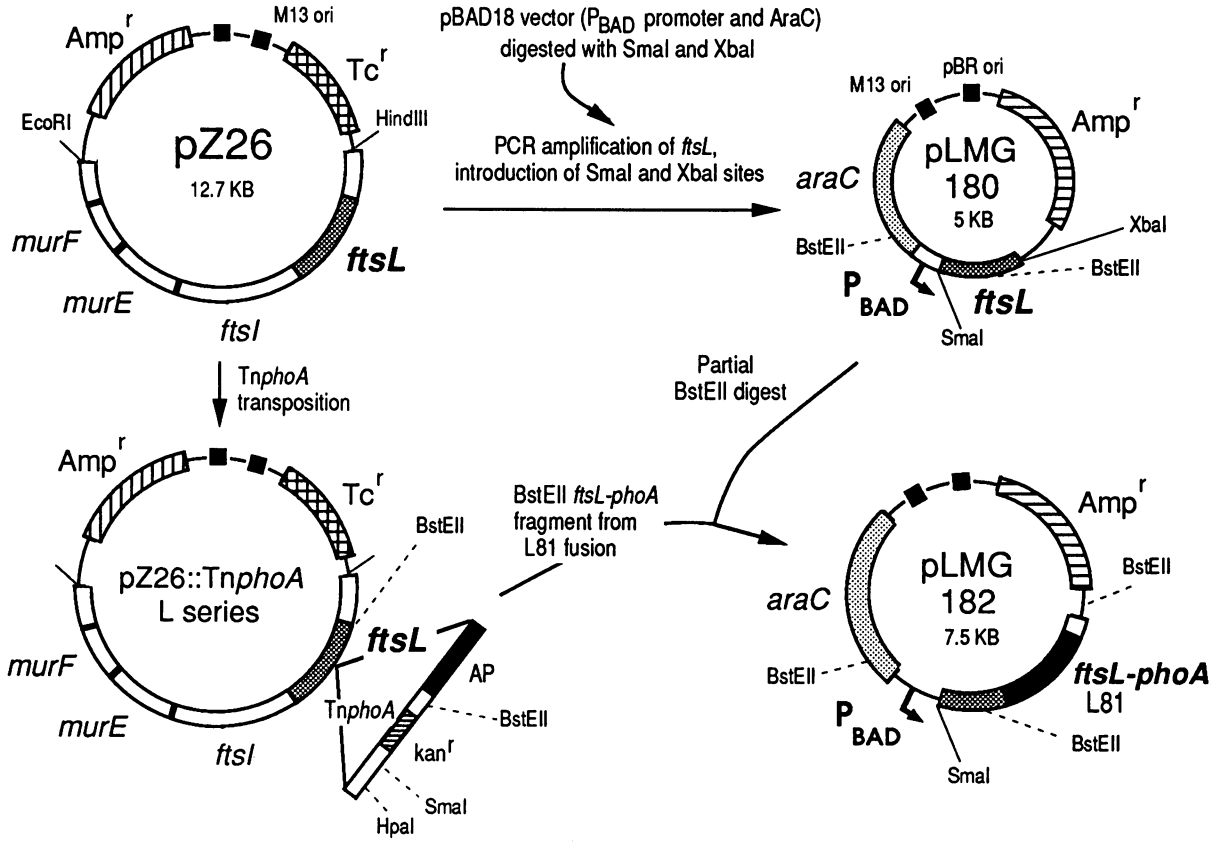

FIG. 1. Plasmid constructs. Plasmid pZ26 was obtained by subcloning a 7.5-kb *Eco*RI-*Hin*dIII fragment from the Clarke-Carbon plasmid pLC26-6 (28) into vector pZ152 (43) digested with the same enzymes. This fragment carries the *ftsI*, *murE*, and *murF* genes. The presence of the *ftsI* gene was confirmed by complementation of the *ftsI*(Ts) allele of strain JJ143 at the nonpermissive temperature. Plasmids pZ26::Tn*phoA*L81, pZ26::Tn*phoA*L88, and pZ26::Tn*phoA*L112 were obtained by transposition of λTn*phoA* into plasmid pZ26 as previously described (2, 20). The insertions were defined by restriction mapping, and the fusion junctions were determined by sequencing (see Fig. 2). Plasmid pLMG180 was constructed by using the polymerase chain reaction (PCR) technique to amplify the DNA corresponding to the *ftsL* gene. The 5′ oligonucleotide was complementary to the region from nucleotides 81 to 96 (Fig. 2) and had a GGG triplet 5′ overhang to be ligated to a *Sma*I site. The 18-mer 3′ oligonucleotide was complementary to the sequence from nucleotides 468 to 485 and contained an *Xba*I site at the end. The 420-bp PCR product was purified, digested with *Xba*I, and cloned into the *Sma*I and *Xba*I sites of the multicloning linker of the pBAD18 vector, which contains the P_{BAD} promoter and the *araC* regulator (to be described elsewhere). Resulting clones were screened by restriction mapping, and positive candidates were tested for complementation of the insertion mutation of strain LMG145 as described in the text. This cloning procedure and complementation for *ftsL* were done in duplicate, starting from two independent PCRs. Plasmid pLMG182 was obtained by subcloning a 1.7-kb *Bst*EII fragment from pZ26::Tn*phoA*L81 into pLMG180 partially digested with the same enzyme. Plasmid pZ26::Tn*phoA*L81 has several *Bst*EII sites (the drawing shows only two sites for simplification). Positive clones, which were blue in XP–L-arabinose plates and white in XP–glucose plates, were further analyzed by restriction digestion. The resulting plasmid contains the L81 fusion under the control of the P_{BAD} promoter and lacks the Kan^r-encoding gene from Tn*phoA*.

was stabilized against transposition by constructing an internal deletion of Tn*phoA* that removed most of the IS*50*R element, as previously described (8). The resulting plasmid, pZ26::Tn*phoA*ΔIS*50*RL81, contains a deletion that extends from the *Sma*I site at position 4434 on the Tn*phoA* map to the *Hpa*I site at position 7551 and retains the kanamycin resistance (Kan^r) gene of Tn*phoA*.

Strain MJC224 [*polA*(Ts)] was transformed with pZ26::Tn*phoA*ΔIS*50*RL81, and integrants of the plasmid into regions of homology with the chromosome were selected by using a low concentration of ampicillin (30 μg/ml) at the nonpermissive temperature for plasmid replication (42°C). The plasmid insertion was indicated by the pale blue color of the colonies on XP plates, since the *polA*$^+$ isogenic strain containing the unintegrated multicopy plasmid gives dark blue colonies. P1 lysates were prepared from 10 pale blue colonies. A pair of *polA*$^+$ *leu*::Tn*10* recipient strains, one with pZ26 (LMG97) and the other without the plasmid (MJC122), were transduced to Kan^r *leu*$^+$ (about 80% linked to *ftsI*). Numerous transductants were obtained in both strains. In the plasmidless strain, dark blue colonies segregated from the parental pale blue strain, suggesting that the entire plasmid, still integrated into the chromosome, was being excised. To select for those cells with chromosomes in which the plasmid had excised leaving behind the Tn*phoA*ΔIS*50*RL81 insertion, pale blue colonies were streaked on high-ampicillin (300 μg/ml) plates several times. P1 lysates were prepared from three of these pale blue colonies (LMG83), and again Kan^r *leu*$^+$ or just *leu*$^+$ transductants were selected in crosses to a *leu*::Tn*10* recipient strain containing plasmid pZ26 (LMG97) or no plasmid (MJC122). Kan^r *leu*$^+$ transductants were obtained in the strain containing the pZ26 plasmid (*ftsL* plus flanking genes), while we failed to observe any Kan^r *leu*$^+$ transductant in the

TABLE 2. AP and specific activities of FtsL-AP fusions

Strain	Plasmid	AP activity (U)[a]		Sp act[b]
		NZY broth	M63	
LMG171	pZ26	0.1	0.2	NT (0.1)
LMG172	pZ26::Tn*phoA*L81	37	120	1.4 (140)
LMG173	pZ26::Tn*phoA*L88	33	141	1.4 (145)
LMG174	pZ26::Tn*phoA*L112	32	89	1.3 (80)
LMG175	pZQ::Tn*phoA80*	16	42	1.2 (50)[c]
MPh42	None; chromosomal wild-type AP	337	1,500	1.0 (1,200)
LMG177	pLMG182 (P_{BAD}-*ftsL-phoA*L81)	380	1,653	NT

[a] AP activity (see Materials and Methods) was determined on duplicate cultures of the indicated strains grown to mid-logarithmic phase at 37°C in rich or minimal medium containing 400 μg of ampicillin per ml (except for MPh42, for which no ampicillin was used). Data represent the average AP units of at least three independent experiments. The average fold overproduction values of the FtsL-AP fusions in pZ26 were 9 ± 0.7-fold in rich medium and 22 ± 6.5-fold (L112) to 29 ± 5.0-fold (L81 and L88) in minimal medium. For the L81 fusion expressed from plasmid pLMG182 (see Materials and Methods), fold overproduction values of 386 ± 30-fold (rich medium) and 1,654 ± 132-fold (minimal medium) were estimated. These values were compared with the activity of the chromosomal *ftsL-phoA* insertion, which has an average AP activity of 4 ± 0.4 U (see the text) and was assumed to represent the wild-type levels of FtsL.

[b] Specific activities were obtained from experiments described in the legend to Fig. 3. Quantification of the amounts of protein fusions and AP and calculations of specific activities were done as described in Materials and Methods. Numbers in parentheses indicate the AP activities of the cultures used for Fig. 3. NT, not tested.

[c] This FtsQ-AP fusion was included as a control. Its AP specific activity has been previously determined to be 1.4 U (8).

plasmidless strain. The frequency of cotransduction obtained by scoring Kan^r colonies among the *leu*$^+$ transductants was 85%.

The *ftsL*::Tn*phoA*ΔIS*50*RL81 insertion was introduced into the *pcnB* mutant strain MJC98/pLMG180 by P1 transduction using lysates of LMG83. Mutant LMG89 was then obtained by selecting for Kan^r on 0.2% L-arabinose plates and screening for absence of growth on 0.2% glucose plates.

Overproduction of FtsL and the FtsL-AP L81 fusion. *ftsL*$^+$ strains with plasmids pLMG180 and pLMG182 were used (Fig. 1). These plasmids carry *ftsL* and the *ftsL-phoA* L81 fusion, respectively, under the control of the arabinose promoter. The extent of induction from this promoter depends on the concentration of L-arabinose, which in these experiments was 0.2%. Overnight cultures of strains LMG148 and LMG177 grown in NZY medium (without L-arabinose) at 37°C were diluted and grown to 2 × 10^7 cells per ml in the same medium. The culture was then divided into two subcultures: 0.2% L-arabinose was added to one, and both were incubated at 37°C and cultured for 6 h more. At 2-h intervals, 0.5-ml fractions were withdrawn from the cultures and fixed with 3.7% formaldehyde for microscopic examination. The growth rate was monitored by measuring the absorbance of cultures in a Klett-Summerson colorimeter with a green filter. Overproduction in minimal medium was performed similarly. Cultures were first grown in 0.2% glycerol-minimal medium, shifted to inducing conditions by addition of 0.2% L-arabinose, and grown for 8 h more. Constitutive expression of *ftsL* in strain LMG145 (FtsL$^-$/pLMG180) was similar, except that the inducer (0.2% L-arabinose) was always present.

Steady-state AP levels in strain LMG177(pLMG182) were determined in log-phase cultures 4 mass doublings after the shift to inducing conditions (Table 2). This was approximately 2.5 h after the shift in rich medium and 4.5 h after the shift in minimal medium.

Photomicroscopy. Cells were visualized and photographed, using phase-contrast microscopy (8). The samples used for photomicroscopy were fixed by addition of 3.7% formaldehyde and kept at 4°C for several days. Average cell length was estimated by comparing cells to a 10-μm grid in photographs printed at the same magnification.

RESULTS

Isolation and characterization of Tn*phoA* insertions in the min 2 region of the *E. coli* chromosome. To identify new cell division genes that encode cell envelope proteins, we used Tn*phoA* transposition to a plasmid carrying DNA from the min 2 cell division cluster of *E. coli*. The Tn*phoA* transposon has been extensively used as a probe for protein export and topology (21). This approach, based on the observation that AP is active only when exported to the periplasm, allows generation of AP fusions by random insertion of the Tn*phoA* transposon. Enzymatically active fusions which correspond to those in which AP is fused to exported proteins or to exported domains of membrane proteins may then be identified (7, 20).

We generated Tn*phoA* insertions into plasmid pZ26 (2), which contains a 7.5-kb fragment derived from the min 2 region of the *E. coli* chromosome carrying the *ftsI*, *murE*, and *murF* genes and about 2 kb of additional DNA (28) (Fig. 1). Several classes of Kan^r, active AP fusions were obtained on this plasmid, including fusions to the *ftsI* gene. We further characterized a class of fusions that mapped 5′ to *ftsI* (2). DNA sequencing revealed that in two fusions of this class, L81 and L88 (Fig. 2), the *phoA* gene was fused to an open reading frame (ORF) immediately preceding the *ftsI* gene (27). The junction of fusion L112, however, was beyond the proposed termination codon for the ORF and was out of frame with respect to it (Fig. 2). Careful sequencing around the fusion junctions revealed that this inconsistency was due to an error in the published sequence (27), which has an extra A at position 426 (Fig. 2). Lack of this base, as indicated in our sequence, shifts the frame of the ORF, resulting in the addition of 11 residues to the inferred protein. It also places fusion L112 within the ORF in a frame consistent with its AP activity. Comparison of our sequence with a recently sequenced portion of the min 2 region (directly submitted to the EMBL gene bank by J. Ayala and assigned accession no. X55034) indicates 100% identity to the ORF. The rectified ORF can code for a protein of 13.6 kDa and 121 residues. We named the gene defined by this ORF *ftsL*, because mutations in it showed defects in cell division (see below).

Determination of the *ftsL-phoA* fusion junctions revealed

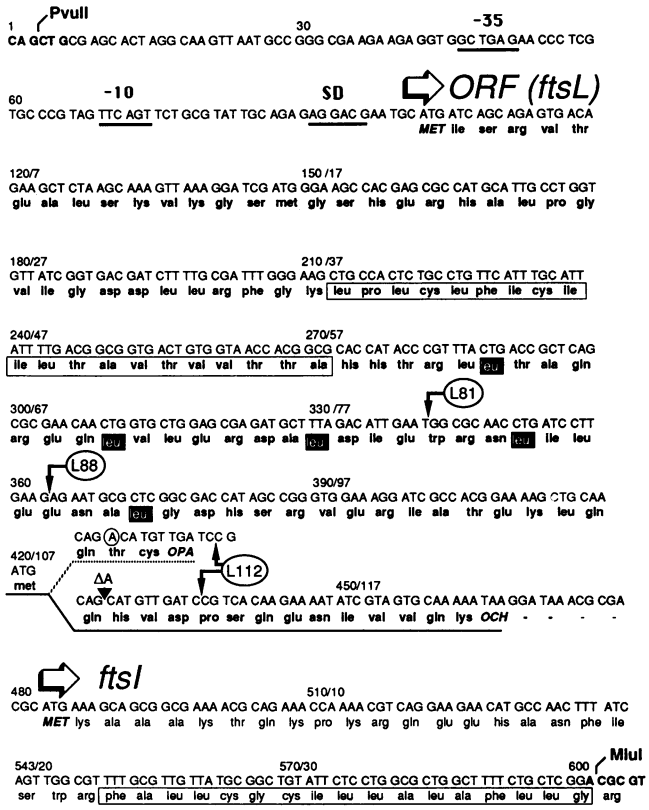

FIG. 2. Sequence of the ORF (*ftsL*) located upstream of the *ftsI* gene. The *ftsL* ORF was sequenced, as described in Materials and Methods, from plasmids containing the L81, L88, and L112 fusions. The sequenced region extends from nucleotides 179 to 542. The rest of the sequence from nucleotides 1 to 178 and 543 to 607 is that of Nakamura et al. (27). Putative −35, −10, and Shine-Dalgarno (SD) sequences are indicated (27). Numbers above the nucleotide sequence correspond to DNA positions/amino acids. The open arrows point to the beginning of the ORF (the *ftsL* gene) and the *ftsI* gene. The inferred amino acid sequence of the ORF is shown in bold type below the nucleotide sequence. Boxed residues correspond to membrane-spanning segments. The junctions of the L81, L88, and L112 fusions (encircled) are shown by solid arrows. The dotted line after Met-107 corresponds to the previously published sequence (27), with an extra A at position 426 (encircled) and an inferred protein of 110 residues. The upper arrow from fusion L112 shows the out-of-frame junction for fusion L112 according to this sequence. The solid line underlines our sequence, from which the A-426 is deleted (ΔA) and a 121-amino-acid protein is inferred. The shaded leucine residues designate the five heptads characteristic of leucine zippers.

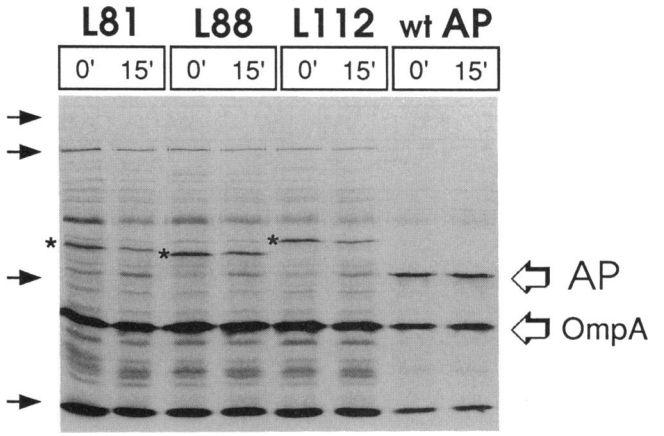

FIG. 3. Relative amounts of FtsL-AP fusion proteins and wild-type AP. pZ26 derivative plasmids containing the FtsL-AP fusions were transformed into strain LMG170 (PhoA$^+$ DegP$^-$). These strains and MPh42 (PhoA$^+$ DegP$^-$) were grown to the log phase at 37°C in M63 glycerol-minimal medium, labeled with 30 μCi of [^{35}S]methionine per ml for 1 min (pulse, 0′), and chased for 15 min by addition of 0.06% unlabeled methionine (chase, 15′). Before labeling, 1-ml fractions were taken from the cultures to assay AP activity (Table 2). Labeled samples were immunoprecipitated with serum against AP and OmpA and analyzed by 10% PAGE as previously described (36). Samples correspond to equivalent amounts of cells, except for lanes with wild-type (wt) AP, in which only one-fifth of the samples were loaded. The positions of the AP and OmpA bands are indicated, as are those of the FtsL-AP fusion proteins (asterisks). The molecular mass standards (arrows to the left) were, from the top, phosphorylase *b* (97.4 kDa), serum albumin (66.2 kDa), ovalbumin (45.0 kDa), and carbonic anhydrase (31.0 kDa). Quantification of the amount of protein in the gel and calculation of the specific activities of the fusions are described in Materials and Methods and Table 2. Protein fusion L88 behaves anomalously and runs faster than the smaller fusion L81.

that fusions were located in the C-terminal region of the FtsL protein, at residues 81, 88, and 112 (Fig. 2). Strains carrying each of the three fusions produced approximately 35 U of AP activity in rich medium and higher AP activity (89 to 141 U) in minimal medium (Table 2). The strain harboring fusion 112, which lacks only the last 10 residues from FtsL, exhibited lower levels of AP activity in minimal medium than did the other two. This difference was found to be due to loss of the plasmid carrying this fusion (PZ26::Tn*phoA*L112), which is highly unstable (data not shown). Additionally, strains carrying the L112 fusion grew at a reduced rate in minimal medium and produced filaments (see below). These observations suggest that expression of the L112 fusion in minimal medium is deleterious to the cell. Expression of the other two *ftsL-phoA* fusions from plasmid pZ26 or of wild-type *ftsL* and flanking genes from the same plasmid did not seem to interfere with normal cell functions, as judged by lack of production of cell filaments.

Hydropathy analysis of the FtsL protein (Kyte and Doolittle algorithm; PC/GENE program from IntelliGenetics, Inc.) revealed a 20-amino-acid hydrophobic stretch in the first half of the protein, from residues 38 to 57 (Fig. 2), which could correspond to a membrane-spanning segment. All three AP fusion junctions were located C terminal to this hydrophobic stretch. The specific AP activities of the FtsL-AP fusions were comparable to that of wild-type AP (Table 2 and Fig. 3), indicating that AP is efficiently translocated across the cytoplasmic membrane in these fusions. These findings suggest that the hydrophobic segment of the FtsL protein corresponds to a strong periplasmic export signal.

Subcellular localization of the FtsL-AP fusions and a topological model for the FtsL protein. When strains harboring the shortest (L81) and largest (L112) fusions (LMG172 and LMG174, respectively) were subjected to subcellular fractionation (see Materials and Methods), the fusion proteins were found exclusively in the cytoplasmic membrane fraction (Fig. 4A). This finding strongly suggests that the wild-type FtsL protein is also localized to this subcellular compartment.

We propose a topological model (20) for the FtsL protein (Fig. 4B): the 121-residue protein possesses a 37-amino-acid cytoplasmic amino-terminal domain, a 20-amino-acid mem-

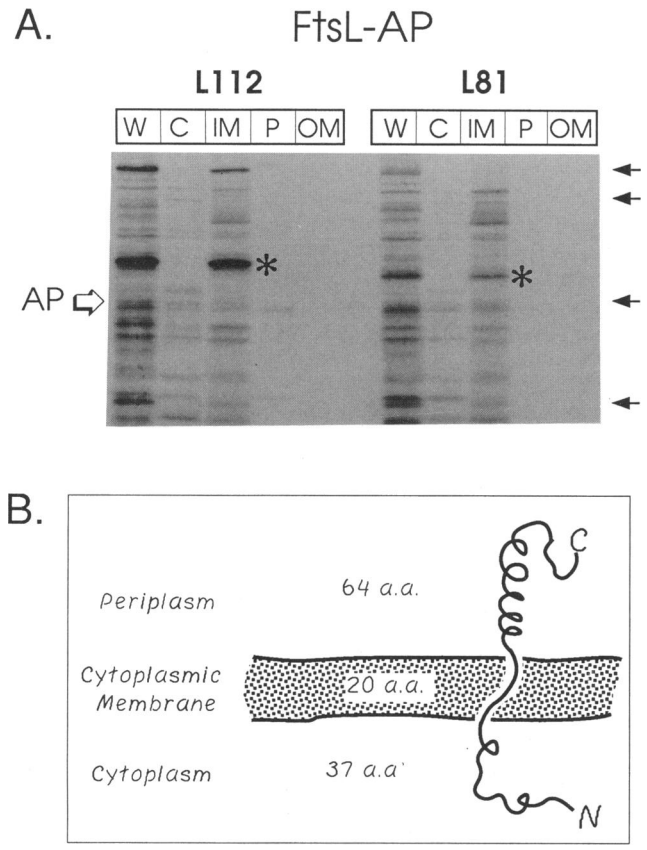

FIG. 4. Subcellular localization of FtsL-AP fusions and topological model of the FtsL protein. (A) Strains LMG172 and LMG174, containing plasmids pZ26::Tn*phoA*L112 and pZ26::Tn*phoA*L81, respectively, were grown, labeled, fractionated, immunoprecipitated, and analyzed by PAGE and fluorography as described in Materials and Methods. The positions of the AP band (open arrow) and the FtsL-AP fusions (asterisks) are indicated. The molecular mass markers (solid arrows) were as described in the legend to Fig. 3. Lanes: W, whole cells; C, cytoplasm; IM, inner membrane; P, periplasm; OM, outer membrane. Lane W was reconstituted from the rest of the fractions. (B) Topology model of the FtsL protein. The drawing represents the proposed model for the topology of FtsL. See the text for details. a.a., amino acids.

brane-spanning segment (from 38 to 57), and a 64-amino-acid periplasmic carboxy-terminal domain (from 58 to 121). This model is supported by the position and high specific activity of FtsL-AP fusions, which indicate that the carboxy-terminal part of the protein, after residue 81, is localized to the periplasm. Furthermore, the FtsL protein does not contain sequence elements found in cleavable signal sequences (40), and inhibition of the SecA export pathway by sodium azide treatment (29) did not cause accumulation of precursors of the FtsL-AP fusions (data not shown). Thus, these results strongly suggest that the *ftsL* gene encodes a simple bitopic cytoplasmic membrane protein.

Essentiality, null phenotype, and abundance of the *ftsL* gene product. To determine the phenotype caused by a null mutation in *ftsL*, we used an *ftsL-phoA* fusion as an insertion mutation in *ftsL*. The shortest *ftsL-phoA* (Kan^r) fusion contained in pZ26 (L81) was crossed into the chromosomal wild-type *ftsL* in a *polA*(Ts) background. Plasmid pZ26::Tn*phoA*L81 was previously stabilized by an IS*50*R deletion to prevent transposition (see Materials and Methods). Selection for excision of the plasmid was applied, and colonies were screened for those in which the wild-type *ftsL* gene was carried on the plasmid and the *ftsL-phoA* fusion remained on the chromosome (see Materials and Methods). P1 transduction using the closely linked *leu* marker was employed to verify the chromosomal location of the *ftsL-phoA* (Kan^r) insertion. When P1 lysates were prepared from these cells (LMG83) and used to transduce the *leu*$^+$ marker to a Leu$^-$ Kan^s strain harboring pZ26 (LMG97), the Kan^r marker was cotransduced at a frequency of 85%. This is the expected cotransduction frequency for *leu* and *ftsL*, given their distance apart on the chromosome and the cotransduction frequency for an *ftsI*(Ts) allele and *leu*, which we found to be 80%.

The essentiality of the *ftsL* gene was then tested by P1 transduction of the *leu*$^+$ marker of the chromosomal *ftsL-phoA* insertion mutant (LMG83) into a *leu* Kan^s recipient strain carrying no plasmid (MJC122) or the pZ26 plasmid (LMG97), which carries *ftsL* and three more genes from the min 2 region. When the recipient strain carrying pZ26 was transduced to *leu*$^+$, we were able to obtain Kan^r cotransductants at a frequency of 82 to 88%. In contrast, no Kan^r cotransductants were obtained when the transduction was performed with the strain without the plasmid. Thus, the cells carrying the insertion mutation were unable to survive unless the wild-type *ftsL* gene (plus flanking sequences) was supplied in *trans* on pZ26. This result indicates that the L81 chromosomal insertion is lethal.

Next, we examined whether the lethality of the *ftsL*::Tn*phoA*L81 insertion can be complemented by expression of *ftsL* only. For this purpose, we constructed a vector containing the tightly regulated promoter from the arabinose operon, the P_{BAD} promoter, and cloned a fragment carrying only the *ftsL* gene into this vector. The resulting plasmid, pLMG180 (Fig. 1), has *ftsL* under the control of P_{BAD} and AraC, a positive and negative regulator of the promoter. The *ftsL* gene could then be expressed in the presence of the inducer L-arabinose or repressed in the absence of inducer or in the presence of glucose. Carson et al. (8) have previously demonstrated the usefulness of this system to effectively turn off gene expression for a cell division gene. They showed that the level of expression of *ftsQ* from P_{BAD} under repressing conditions is so low that it fails to express the 20 to 40 molecules of FtsQ protein per cell needed to complement *ftsQ* insertion mutations.

The essentiality test was then repeated using the above-described P1 lysates (LMG83), this time transducing *leu*$^+$ to a strain harboring pLMG180 (LMG148). When the *ftsL-phoA* chromosomal insertion was transduced into this strain in medium supplemented with 0.2% L-arabinose (at 37°C), Kan^r cotransductants were observed at a frequency of 85%. These cotransductants exhibited normal size and cell shape. However, when the recipient was a strain with no plasmid, with the parent P_{BAD} vector (with or without inducer), or with the P_{BAD} *ftsL* plasmid in medium supplemented with 0.2% glucose, no Kan^r cotransductants were obtained among the *leu*$^+$ colonies. Similar results were obtained when this essentiality test was performed at 29 or 42°C in rich or minimal medium.

These results indicate that the *ftsL-phoA* insertion mutation is lethal and that this phenotype can be complemented by the *ftsL* gene alone. Furthermore, they indicate that the essential *ftsI* gene and downstream genes are expressed from the chromosome in the presence of the insertion, since lack of *ftsI* is lethal (35). Whether these genes are transcribed

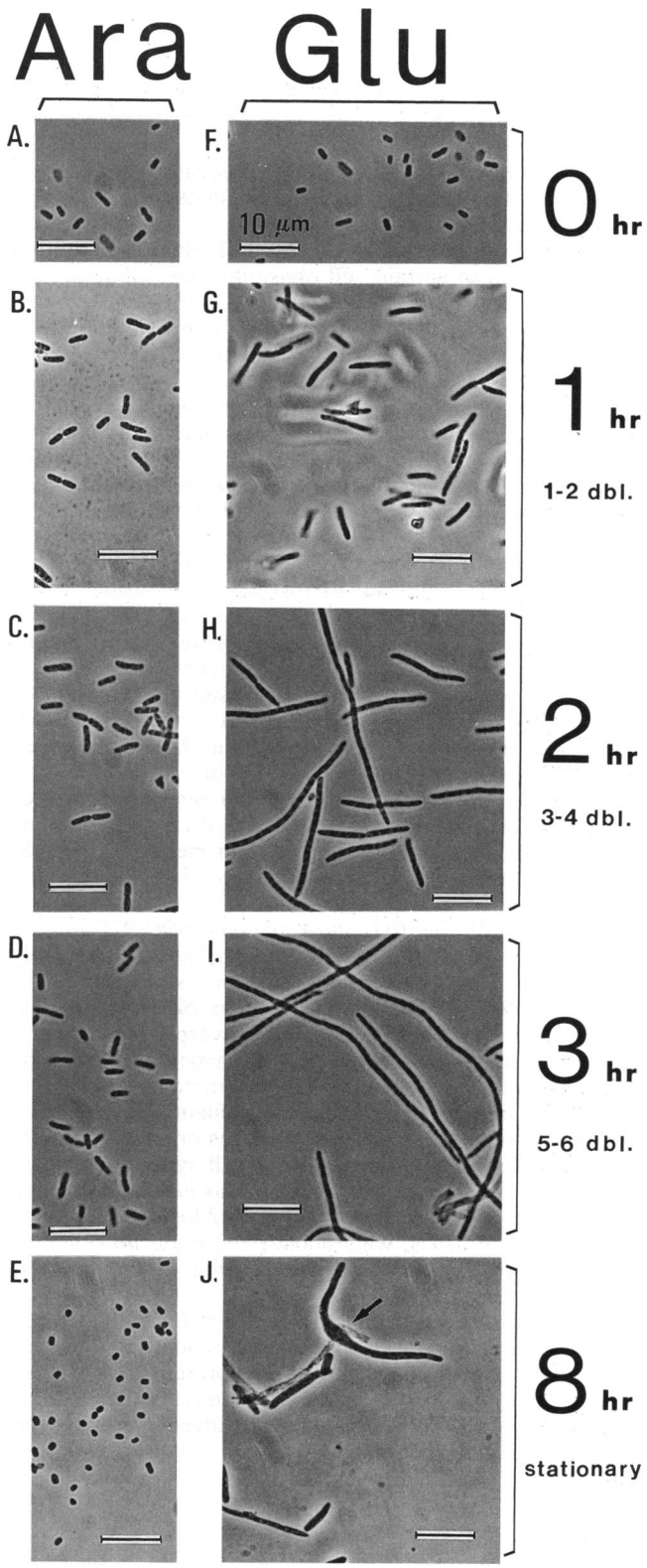

FIG. 5. FtsL-null phenotype. Strain LMG145 (*ftsL*::Tn*phoA*L 81ΔIS*50*R/pLMG180) was grown to stationary phase at 37°C in rich broth containing 0.1% L-arabinose and ampicillin. Cultures were then washed, diluted 1:100 in rich medium lacking ampicillin and containing 0.1% L-arabinose (A to E) or 0.2% glucose (F to J), and grown for 12 h at 37°C. Every 30 min, 1-ml fractions were withdrawn from the cultures and cells were fixed and examined under phase-contrast microscopy. Additionally, the growth rates of the cultures were monitored by measuring absorbance in a Klett-Summerson photocolorimeter, and the doubling time (28 min) was calculated. Only cells corresponding to 0, 1, 2, 3, and 8 h after the shift to repressing conditions are shown. Cells from 0- and 1-h samples were concentrated by centrifugation. Cellular suspensions were fixed and photographed as indicated in Materials and Methods. dbl., mass doublings. Bars, 10 μm.

from the end of the Tn*phoA*ΔIS*50*R insertion or the insertion is upstream of a promoter included within *ftsL* is not known. It appears that expression of these chromosomal genes downstream from the *ftsL-phoA* insertion is not drastically altered, since complementation of the insertion by *ftsL* alone gives a phenotype indistinguishable from that of the wild type (Fig. 5A to E). Additionally, the lethality of the *ftsL-phoA* insertion is likely due to the lack of a complementing copy of *ftsL* rather than expression of the fusion, since expression of the same fusion from the multicopy plasmid pZ26 does not detectably alter cell physiology. Thus, these results strongly suggest that *ftsL* corresponds to an essential gene.

Estimates of the AP activity in the chromosomal fusion provided information on the chromosomal expression levels of *ftsL*. Strains containing the *ftsL-phoA* insertion L81 produced 4.4 (LMG83), 3.5 (LMG145), and 4.2 (LMG142) U of AP activity in rich medium. Remarkably similar levels of expression were observed with *ftsQ-phoA* chromosomal fusions contained in strains MJC251 and MJC252, which produced 3.9 and 4.2 U, respectively. These values had been previously determined and used to estimate that FtsQ is present at 20 to 40 copies per cell (8). Although these calculations are based on indirect measurements and therefore should be considered rough estimates, they do indicate that the copy number of the FtsL protein is quite similar to that of FtsQ and that this corresponds to a very low abundance.

The phenotype of the *ftsL* null mutation indicates that *ftsL* corresponds to a cell division gene. To determine whether the ORF (*ftsL*) located upstream of *ftsI* is involved in the cell division process, the phenotype of the null insertion mutation was studied. Strains LMG145 (Ara^+) and LMG142 (Ara^-) carrying the insertion mutation complemented by pLMG180 were grown to the stationary phase in rich medium supplemented by 0.1% L-arabinose. This concentration of L-arabinose was found to give a good complementation profile, as judged by phase-contrast microscopy of log- and stationary-phase cultures. Under these conditions, the cells looked normal in size and shape (Fig. 5A to E). These parameters were the same in wild-type strains grown in medium containing L-arabinose or glucose (data not shown). When stationary-phase cultures of the insertion mutants grown in L-arabinose-rich medium were washed, diluted, and grown in rich medium supplemented with 0.2% glucose for 5 to 7 h, long, nonseptate cell filaments were observed in the cultures.

This cessation of cell division appears to be fast and efficient. Within only 1 to 2 mass doublings (1 h) after the cultures of LMG145 were diluted and grown in medium containing glucose, most of the cells had stopped dividing and short filaments corresponding to two normal cell lengths were observed (Fig. 5G). After approximately 3 to 4 mass doublings (2 h), filaments corresponding to 4 to 8 cell lengths were then seen (Fig. 5H). At later times, long (6 mass doublings; Fig. 5I) to very long filaments (in stationary phase) which eventually lysed were observed. Prior to lysis,

in stationary-phase cultures a significant proportion of filaments showed an overall increase in diameter, which was irregular along the filament. This resulted in thicker filaments, some with bulges (Fig. 6F) and some wider at one end than the other or irregular in shape (Fig. 5J). Interestingly, while extensive filamentation was taking place during the first 1 to 2 h of FtsL depletion in LMG145 cultures (Fig. 5G and H), the growth rate of these cultures was indistinguishable from that of control strain LMG148 (*ftsL*$^+$) grown in the same conditions (data not shown). After 2 h, however, the slope of the growth curve of the FtsL-depleted cultures began to decrease. Thus, during the early stages of FtsL depletion, cell division is effectively blocked, producing cell filamentation, while cell elongation and growth are basically unaffected by lack of FtsL.

Depletion of FtsL in minimal medium was not as effective as in rich medium. However, plasmid pLMG180 was unstable in cells (LMG145) growing in glycerol-minimal medium, which provided an excellent way to evaluate the *ftsL* null mutation phenotype in cells that had lost the plasmid. These cells produced very long, thin, nonseptate filaments and a few filaments with partial septa. The proportion of filaments was approximately 5 to 20% in cultures growing in medium supplemented with L-arabinose or glucose in the absence of ampicillin (pLMG180 in strain LMG145 is stable in rich medium, even in the absence of ampicillin). Depletion of FtsL in a *pcnB* mutant strain carrying the *ftsL-phoA* insertion mutation (LMG89) was very effective, since the strain readily loses the complementing plasmid pLMG180. The *pcnB* mutation (18a) reduces the copy number of pBR322 and its derivatives and also appears to affect their stability. Subculture of strain LMG89 after overnight growth in minimal medium resulted in formation of long, nonseptate filaments by most of the cells in the culture.

Among the cell filaments produced in minimal medium, a striking feature was observed. A low proportion of the filaments displayed one or more cell extensions, resulting in Y-shaped filaments (Fig. 6).

The extra appendages were observed early in the development of some filaments after 1 or 2 doublings, producing small Y-shaped cells (Fig. 6A) which would later become Y-shaped filaments (Fig. 6B to D). Also, we observed short or long filaments with protruding buds (Fig. 6E) which sometimes extended into an appendage, resulting in wishbone-shaped filaments (Fig. 6C and D). In most cases, this extra appendage seemed to originate at an angle of approximately 120° from the center or near the ends of filaments. It appears that the sites at which the appendages originate correspond to partial or residual septa. Also, the poles of the extra appendage in Y-shaped cells were sometimes seen to bifurcate into two more appendages (Fig. 6B shows a pole with an incipient bifurcation). This morphological change, however, was present in only a very small percentage of the Y-shaped filaments. Interestingly, regularly spaced nucleoids were observed in the tripartite filaments (and normal filaments) (data not shown), suggesting that chromosome segregation had an unusual change in direction at the point of bifurcation of the extra appendage.

The formation of filaments with bulges (Fig. 6F) or irregular thickness (Fig. 5J) or the presence of cells with less frequent morphologies, like lysis bubbles and spheroplasts (data not shown), was observed in depletion experiments in rich or minimal medium (in the presence or absence of ampicillin). In contrast, Y-shaped cells and Y-shaped filaments were observed exclusively during growth in minimal medium. It is possible that there is an intrinsic property of growth in minimal medium that may help the production of certain cell types, like Y-shaped cells. For instance, a slower growth rate could be important for the manifestation of these defects or differences in cell wall composition due to nutrients in the medium may impose additional stress in morphogenetic processes.

These results indicate that the gene located upstream of *ftsI*, the *ftsL* gene, is involved in the cell division process and possibly in morphogenesis.

Additional conditions that affect cell division. Constitutive overexpression of certain cell division genes, namely, *ftsZ* (42) and *minCD* (10), has been shown to alter the cell division process significantly. To examine this situation with *ftsL*, the FtsL protein was overproduced from the arabinose promoter (see Materials and Methods). The expression levels of *ftsL* from this promoter were found to be 96 ± 6-fold and 410 ± 33-fold overproduction in rich and minimal media, respectively. This was estimated from the AP activity levels of the L81 FtsL-AP fusion expressed from the P_{BAD} promoter (pLMG182) (see Materials and Methods and Table 2).

The effect of FtsL overproduction (in FtsL$^+$ or FtsL$^-$ strains) in rich medium was almost negligible, aside from a few short filaments present in the cultures. In minimal medium, however, FtsL overproduction resulted in multiseptate, nonseptate, and Y-shaped filaments. Overexpression of the P_{BAD}-L81 fusion also caused filamentation in minimal medium. Thus, wild-type FtsL and the FtsL-AP L81 fusion are able to exert a negative effect on the cell division process only under conditions of vast overproduction. It is not clear, however, whether overproduction of FtsL specifically interferes with the cell division process or whether a large excess of this particular membrane protein (FtsL) could produce filaments as a secondary, nonspecific effect.

Expression of the *ftsL-phoA* fusions L81 and L88 in plasmid pZ26 (from the *ftsL* promoter) had no detectable effect on the cell division process. In contrast, expression of the largest *ftsL-phoA* fusion (L112) in pZ26 in minimal medium, which is only 22 ± 6.5-fold overproduced, had a number of interesting effects on cell shape. Its phenotype was very similar to that of the *ftsL* null mutation in minimal medium. It induced the formation of filaments, Y-shaped cells and filaments, filaments with bulges or irregular thickness, etc. The proportion of these cell types in a given culture was variable, from 1 to 10%. This is very likely due to loss of the plasmid containing the L112 fusion, which was very unstable. That is, while most (>90%) of the cells had lost the plasmid, all of those still carrying it showed morphological changes.

The variety of conditions under which *ftsL* can induce cell division defects (i.e., lack of *ftsL* expression, *ftsL* overexpression, or expression of *ftsL* fusion proteins), as well as the striking variety of these defects, suggests that FtsL is involved in an important step of the cell division process and possibly in cell morphogenesis.

DISCUSSION

In this report, we describe the identification and preliminary characterization of *ftsL*, a cell division gene localized in the min 2 region of the *E. coli* chromosome. Sequencing of Tn*phoA* insertions in a plasmid carrying DNA from this region showed that *ftsL* maps to an ORF localized immediately upstream of the *ftsI* gene (Fig. 2). Both genes are transcribed in the same direction and are separated by only

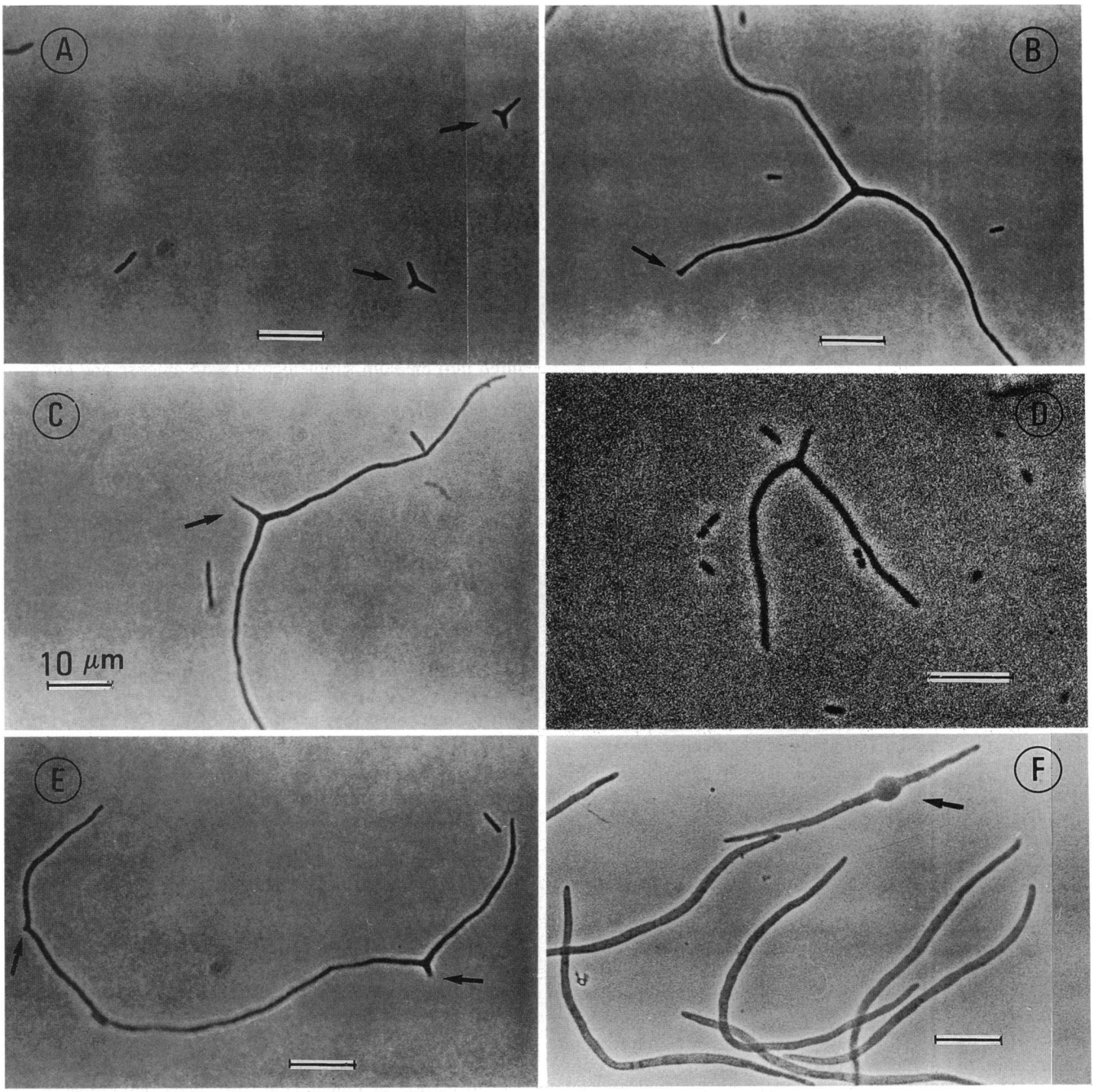

FIG. 6. FtsL-related cellular morphologies. Experiments were performed as described in the legend to Fig. 5, except that cells were grown in minimal medium. (A to E) Examples of different cell morphologies found in cultures of strain LMG145 (*ftsL*::Tn*phoA*L81ΔIS*50*R/pLMG180) grown to stationary phase at 37°C in glycerol-minimal medium supplemented with glucose. Cells had a doubling time of close to 1 h. For photomicroscopy, fixed cell suspensions corresponding to hours 6 and 9 were applied directly to microscope slides. In panel B, 10 μl of fixed cells was spread on a slide covered with a thin layer of 1.5% minimal agar. Panels: A, Y-shaped cells; B, Y-shaped filament with an incipient bifurcation at one pole (arrow); C and D, wishbone-shaped filaments with a small extra appendage (arrow); E, filament with two small protruding buds (arrows); F, FtsL depletion in the insertion mutant strain LMG89 (PcnB$^-$). Experiments were performed in rich medium as indicated in the legend to Fig. 5. Each arrow points to the central bulge present in a filament obtained from an 8-h culture. Bars, 10 μm.

15 bp (instead of 49 bp, as the original DNA sequence suggested [27]). No transcriptional termination sequences are found between the two genes, and consensus promoter sequences upstream of *ftsL* and *ftsI* can be identified (27). These observations suggest that *ftsL* and *ftsI* are part of an operon, where *ftsI* may also be transcribed independently. Ishino et al. (15) have described two mutants obtained by hydroxylamine mutagenesis that were thermosensitive for

cell growth and division and mapped upstream of the *ftsI* gene. Complementation results placed the mutations in the same region as *ftsL*. At the nonpermissive temperature, one mutant formed filamentous cells, whereas the other lysed without forming filaments. Recent evidence indicates that both mutations correspond to alleles of the *ftsL* gene (39a).

The hydropathy profile of FtsL and the analysis and subcellular fractionation of active FtsL-AP fusions (Table 2 and Fig. 3 and 4A) strongly suggest that FtsL is a cytoplasmic membrane protein whose carboxy-terminal domain is efficiently exported to the periplasm. On the basis of these findings, we have proposed a topological model for the FtsL protein (Fig. 4B). According to this model, FtsL is a simple bitopic membrane protein with a single membrane-spanning segment, a 37-amino-acid cytoplasmic amino-terminal domain, and a 64-amino-acid periplasmic C-terminal domain. FtsI (1a, 6) and FtsQ (8, 12), two other cell division proteins encoded in the min 2 cluster, also have simple bitopic membrane topologies. However, these two proteins have short amino-terminal cytoplasmic domains (23 and 24 residues, respectively) and much larger periplasmic carboxy-terminal domains (546 and 227 residues). The periplasmic domain of FtsI contains transpeptidase and transglycosylase enzymatic functions, which are likely related to septum formation (16) and penicillin-binding ability (6). FtsQ does not have a known enzymatic function, but it has been speculated that its periplasmic domain has a direct enzymatic role in cell division (8).

Another feature that FtsL shares with FtsI and FtsQ is the fact that all three proteins are present in very small amounts in the cell. In this study, the abundance of FtsL was estimated to be between 20 and 40 molecules per cell, and similar abundance estimates have been reported for FtsQ (8) and FtsI (34). These common features raise the possibility that these three proteins are part of a stoichiometric membrane-bound complex which functions in the cell division process. Bitopic membrane proteins of this type are potential candidates for signalling molecules that could coordinate periplasmic processes such as peptidoglycan assembly with events in the cytoplasm, such as DNA synthesis or chromosome segregation. A role for this type of signal transduction in bacterial cell division has yet to be established.

The sequence of the periplasmic domain of FtsL exhibits a series of five leucines separated from each other by seven residues (Fig. 2). This structural motif is seen in so-called leucine zipper domains, which are involved in the dimerization of proteins and were originally described in eukaryotic transcriptional regulators (30, 39). Recently, it has been shown that the yeast GCN4 leucine zipper can promote dimerization in the *E. coli* periplasmic space (5), and examples of natural bacterial leucine zippers have been described (22, 32).

The potential FtsL leucine zipper displays some features present in known leucine zippers, such as polar residues at position 4 in each heptad (39). According to the model of Tropsha et al. (39), the leucines and polar residues at position 4 interact at the dimer interface and stabilize the coiled coil by hydrophobic interactions and hydrogen bonding. Additionally, consistent with the secondary structure of leucine zippers, Chou and Fasman analysis of FtsL (PC/GENE program from IntelliGenetics, Inc.) predicts that almost the entire periplasmic domain has a helical structure. However, a characteristic proposed by O'Shea et al. (30), namely, the presence of hydrophobic residues at position 5, does not occur in the FtsL zipper motif.

These observations raise the possibility that FtsL interacts with itself or other proteins to form homo- or heterodimers. However, the functional significance of this zipper sequence in FtsL remains to be demonstrated. We are currently examining this issue.

We disrupted the *ftsL* gene by using an *ftsL-phoA* fusion (fusion L81) as an insertion mutation in *ftsL*. The viability and cell division of this insertion mutant were dependent on the expression of a complementing copy of the *ftsL* gene in *trans*. Thus, we conclude that *ftsL* is a gene whose product is essential for cell viability and division.

The block in cell division resulting from depletion of FtsL occurred rapidly; as early as 1 or 2 mass doublings after the arrest of FtsL synthesis, nonseptate filaments began to form (Fig. 5G). After 3 to 4 mass doublings, long filaments were readily observed (Fig. 5H). This pattern was obtained whenever overnight stationary-phase cultures were directly diluted into medium supplemented with glucose and cultured under repressing conditions. However, when the cells (LMG145) were first grown for 2 generations to early log phase in medium supplemented with L-arabinose and then shifted to repressing conditions, the onset of the division block was retarded. These findings could be explained if, in stationary-phase cultures, FtsL had a shorter half-life or if FtsL were present at low concentrations resulting from depletion of L-arabinose in the cultures.

Overproduction of FtsL resulted in strong cell division defects only when FtsL was overexpressed around 400-fold, while at least 90-fold overexpression produced mild to negligible effects. This suggests that cells are tolerant to high levels of the FtsL protein throughout the cell cycle. Similar results have been reported for overproduction of FtsQ from the arabinose promoter (8).

It is interesting that expression of the L112 fusion from pZ26 in minimal medium (22 ± 6.5-fold overexpression) produced a phenotype very similar to the one observed during depletion of FtsL in the same medium, while expression of the shorter fusion proteins did not. It is possible that the L112 fusion protein has a dominant negative effect under these conditions. The L112 fusion protein contains almost the entire periplasmic domain of FtsL (it lacks only the last 10 residues), which may interact with other proteins via a zipper motif. This fusion may be able to displace wild-type FtsL either by being assembled into a complex of which FtsL is normally part or by titrating out a protein that otherwise interacts with wild-type FtsL. After this step, however, the L112 fusion would be unable to carry out the rest of the normal FtsL functions.

Most of the observed FtsL-related cell morphologies (Fig. 5 and 6) have been previously described in other situations. The formation of bulges (Fig. 6F), lysis bubbles at septal sites, and spheroplasts (data not shown) is reminiscent of a double mutant in PBP2 and PBP3 (3) and inactivation of these two proteins by β-lactam antibiotics (11, 34). Additionally, mutations in the *htrB* gene, whose product is essential at temperatures above 33°C, produce similar bulges (18). Cells and filaments with irregular thickness (Fig. 5J) are similar to those of a *bolA ftsZ* double mutant (1). Mutants whose phenotypes include formation of Y-shaped cells (Fig. 6) have been described in *Klebsiella pneumoniae* (33) and very recently in *Caulobacter crescentus* (7a) and in *E. coli* strains carrying a temperature-sensitive mutation on the *ftsZ* gene [*ftsZ26*(Ts)] (4a). The nature of these FtsL-related altered cell morphologies and division defects (filaments), which in part are similar to those produced by mutant or inactivated PBP proteins, suggests that lack of

FtsL and expression of the L112 fusion have global effects on cell wall structure, possibly due to general weakening.

Thus, the spectrum of phenotypes associated with *ftsL* mutants suggests that *ftsL* is involved in both cell division and peptidoglycan physiology or in some coupling between the two processes. Similar conclusions have been reached by Veki et al. (39a) in their studies with two Ts alleles of *ftsL*, although they interprete the cell lysis phenotype of one of these mutants (*lts-33* [15]) as indicating a primary role for *ftsL* (*mraR*) in elongation and morphogenesis. It is interesting to note that Bi and Lutkenhaus (4a) have recently described two mutations in the cell division gene *ftsZ* [*ftsZ*(Rsa) and *ftsZ261*(Cs)] that cause cell lysis at the nonpermissive temperature. They suggest that at least in the case of the Cs mutant, which has an altered FtsZ ring structure, lysis is due to a decrease in coordination of the mutant FtsZ ring and the septal biosynthetic machinery. Some of the features of the FtsL protein that we have described here may help in finding target molecules with which FtsL interacts and in further defining its role in cell division and morphogenic processes.

ACKNOWLEDGMENTS

We thank members of the Beckwith laboratory and Dominique M. Belin for comments on the manuscript. We are grateful to Mike Carson for generously providing strains, plasmids, and helpful advice. We thank Yves V. Brun and Lucy Shapiro for communicating results prior to publication. We also thank Terri Luna for technical assistance and Ann McIntosh for administrative assistance.

This work was supported by grant MV-5U from the American Cancer Society. L.-M.G. is a Merck Sharp & Dohme Postdoctoral Fellow. J.B. is an American Cancer Society Research Professor.

REFERENCES

1. **Aldea, M., C. Hernandez-Chico, A. G. de la Campa, S. R. Kushner, and M. Vicente.** 1988. Identification, cloning, and expression of *bolA*, an *ftsZ*-dependent morphogene of *Escherichia coli*. J. Bacteriol. **170:**5169–5176.

1a. **Barondess, J. J., and J. Beckwith.** Unpublished data.

2. **Barondess, J. J., M. Carson, L.-M. Guzman-Verduzco, and J. Beckwith.** 1991. Alkaline phosphatase fusions in the study of cell division genes. Res. Microbiol. **142:**295–299.

3. **Begg, K. J., and W. D. Donachie.** 1985. Cell shape and division in *Escherichia coli*: experiments with shape and division mutants. J. Bacteriol. **163:**615–622.

4. **Bi, E., and J. Lutkenhaus.** 1991. FtsZ ring structure associated with division in *Escherichia coli*. Nature (London) **354:**161–164.

4a. **Bi, E., and J. Lutkenhaus.** 1992. Isolation and characterization of *ftsZ* alleles that affect septal morphology. J. Bacteriol. **174:**5414–5423.

5. **Blondel, A., and H. Bedouelle.** 1991. Engineering the quaternary structure of an exported protein with a leucine zipper. Prot. Eng. **4:**457–461.

6. **Bowler, L. D., and B. G. Spratt.** 1989. Membrane topology of penicillin-binding protein 3 of *Escherichia coli*. Mol. Microbiol. **3:**1277–1286.

7. **Boyd, D., C. Manoil, and J. Beckwith.** 1987. Determinants of membrane protein topology. Proc. Natl. Acad. Sci. USA **84:** 8525–8529.

7a. **Brun, Y. V., and L. Shapiro.** Personal communication.

8. **Carson, M. J., J. Barondess, and J. Beckwith.** 1991. The FtsQ protein of *Escherichia coli*: membrane topology, abundance, and cell division phenotypes due to overproduction and insertion mutations. J. Bacteriol. **173:**2187–2195.

8a. **Cormack, B.** Personal communication.

9. **de Boer, P. A. J., W. R. Cook, and L. I. Rothfield.** 1990. Bacterial cell division. Annu. Rev. Genet. **24:**249–274.

10. **de Boer, P. A. J., R. E. Crossley, and L. I. Rothfield.** 1992. Roles of MinC and MinD in the site-specific septation block mediated by the MinCDE system of *Escherichia coli*. J. Bacteriol. **174:** 63–70.

11. **Donachie, W. D., and A. C. Robinson.** 1987. Cell division: parameter values and the process, p. 1578–1593. *In* F. C. Neidhardt (ed.), *Escherichia coli* and *Salmonella typhimurium*: cellular and molecular biology. American Society for Microbiology, Washington, D.C.

12. **Dopazo, A., P. Palacios, M. Sanchez, J. Pla, and M. Vicente.** 1992. An amino-proximal domain required for the localization of FtsQ in the cytoplasmic membrane, and for its biological function in *Escherichia coli*. Mol. Microbiol. **6:**715–722.

13. **Guzman-Verduzco, L.-M., and Y. M. Kupersztoch.** 1990. Export and processing analysis of a fusion between the extracellular heat-stable enterotoxin and the periplasmic B subunit of the heat-labile enterotoxin in *Escherichia coli*. Mol. Microbiol. **4:**253–264.

14. **Hirota, Y., A. Ryter, and F. Jacob.** 1968. Thermosensitive mutants of *E. coli* affected in the process of DNA synthesis and cellular division. Cold Spring Harbor Symp. Quant. Biol. **33:** 677–693.

15. **Ishino, F., H. K. Jung, M. Ikeda, M. Doi, M. Wachi, and M. Matsuhashi.** 1989. New mutations *fts-36*, *lts-33*, and *ftsW* clustered in the *mra* region of the *Escherichia coli* chromosome induce thermosensitive cell growth and division. J. Bacteriol. **171:**5523–5530.

16. **Ishino, F., and M. Matsuhashi.** 1981. Peptidoglycan synthetic enzyme activities of highly purified penicillin-binding protein 3 in *Escherichia coli*: a septum-forming reaction sequence. Biochem. Biophys. Res. Commun. **101:**905–911.

17. **Jones, C., and I. B. Holland.** 1985. Role of the SulB (FtsZ) protein in division inhibition during the SOS response in *Escherichia coli*: FtsZ stabilizes the inhibitor SulA in maxicells. Proc. Natl. Acad. Sci. USA **82:**6045–6049.

18. **Karow, M., O. Fayet, A. Cegielska, T. Ziegelhoffer, and C. Georgopoulos.** 1991. Isolation and characterization of the *Escherichia coli htrB* gene, whose product is essential for bacterial viability above 33°C in rich media. J. Bacteriol. **173:**741–750.

18a. **Lopilato, J., S. Bortner, and J. Beckwith.** 1986. Mutations in a new chromosomal gene of *Escherichia coli*, *pcnB*, reduce plasmid copy number of pBR322 and its derivatives. Mol. Gen. Genet. **205:**285–290.

19. **Lutkenhaus, J.** 1990. Regulation of cell division in *E. coli*. Trends Genet. **6:**22–25.

20. **Manoil, C., and J. Beckwith.** 1986. A genetic approach to analyzing membrane protein topology. Science **233:**1403–1408.

21. **Manoil, C., J. J. Mekalanos, and J. Beckwith.** 1990. Alkaline phosphatase fusions: sensors of subcellular location. J. Bacteriol. **172:**515–518.

22. **Maxon, M. E., J. Wigboldus, N. Brot, and H. Weissbach.** 1990. Structure-function studies on *Escherichia coli* MetR protein, a putative prokaryotic leucine zipper protein. Proc. Natl. Acad. Sci. USA **87:**7076–7079.

23. **Michaelis, S., H. Inouye, D. Oliver, and J. Beckwith.** 1983. Mutations that alter the signal sequence of alkaline phosphatase in *Escherichia coli*. J. Bacteriol. **154:**366–374.

24. **Miller, J. H.** 1972. Experiments in molecular genetics. Cold Spring Harbor Laboratory, Cold Spring Harbor, N.Y.

25. **Miyakawa, T., H. Matsuzawa, M. Matsuhashi, and Y. Sugino.** 1972. Cell wall peptidoglycan mutants of *Escherichia coli* K-12: existence of two clusters of genes, *mra* and *mrb*, for cell wall peptidoglycan biosynthesis. J. Bacteriol. **112:**950–958.

26. **Mukherjee, A., and W. D. Donachie.** 1990. Differential translation of cell division proteins. J. Bacteriol. **172:**6106–6111.

27. **Nakamura, M., I. N. Maruyama, M. Soma, J.-I. Kato, H. Suzuki, and Y. Hirota.** 1983. On the process of cellular division in *Escherichia coli*: nucleotide sequence of the gene for penicillin-binding protein 3. Mol. Gen. Genet. **191:**1–9.

28. **Nishimura, Y., Y. Takeda, A. Nishimura, H. Suzuki, M. Inouye, and Y. Hirota.** 1977. Synthetic ColE1 plasmids carrying genes for cell division in *Escherichia coli*. Plasmid **1:**67–77.

29. **Oliver, D. B., R. J. Cabelli, K. M. Dolan, and G. P. Jarosik.** 1990. Azide-resistant mutants of *Escherichia coli* alter the SecA protein, an azide-sensitive component of the secretion machin-

ery. Proc. Natl. Acad. Sci. USA **87**:8227–8231.
30. **O'Shea, E. K., R. Rutkowski, and P. S. Kim.** 1989. Evidence that the leucine zipper is a coiled coil. Science **243**:538–542.
31. **Robinson, A. C., D. J. Kenan, G. F. Hatfull, N. F. Sullivan, R. Spiegelberg, and W. D. Donachie.** 1984. DNA sequence and transcriptional organization of essential cell division genes *ftsQ* and *ftsA* of *Escherichia coli*: evidence for overlapping transcriptional units. J. Bacteriol. **160**:546–555.
32. **Sasse, D. S., and J. D. Gralla.** 1990. Role of eukaryotic-type functional domains found in the prokaryotic enhancer receptor factor sigma 54. Cell **62**:945–954.
33. **Satta, G., and R. Fontana.** 1974. Characterization of a conditional mutant with altered envelope showing pH-dependent morphology and temperature dependent division. J. Gen. Microbiol. **80**:51–63.
34. **Spratt, B. G.** 1975. Distinct penicillin-binding proteins involved in the division, elongation and shape of Escherichia coli K-12. Proc. Natl. Acad. Sci. USA **72**:2999–3003.
35. **Spratt, B. G.** 1977. Properties of the penicillin-binding proteins of *Escherichia coli* K-12. Eur. J. Biochem. **72**:341–352.
36. **Strauch, K. L., and J. Beckwith.** 1988. An *Escherichia coli* mutation preventing degradation of abnormal periplasmic proteins. Proc. Natl. Acad. Sci. USA **85**:1576–1580.
37. **Tetart, F., R. Albigot, A. Conter, E. Mulder, and J.-P. Bouche.** 1992. Involvement of FtsZ in coupling of nucleoid separation with septation. Mol. Microbiol. **6**:621–627.
38. **Tormo, A., J. A. Ayala, M. A. de Pedro, M. Aldea, and M. Vicente.** 1986. Interaction of FtsA and PBP3 proteins in the *Escherichia coli* septum. J. Bacteriol. **166**:985–992.
39. **Tropsha, A., J. P. Bowen, F. K. Brown, and J. S. Kizer.** 1991. Do interhelical side chain-backbone hydrogen bonds participate in formation of leucine zipper coiled coils? Proc. Natl. Acad. Sci. USA **88**:9488–9492.

39a. **Veki, M., M. Wachi, H. K. Jung, F. Ishino, and M. Matsuhashi.** 1992. *Escherichia coli mraR* gene involved in cell growth and division. J. Bacteriol. **174**:7841–7843.

40. **von Heijne, G.** 1990. The signal peptide. J. Membr. Biol. **115**:195–201.
41. **Wang, X., P. A. J. de Boer, and L. I. Rothfield.** 1991. A factor that positively regulates cell division by activating transcription of the major cluster of essential cell division genes of *Escherichia coli*. EMBO J. **10**:3363–3372.
42. **Ward, J. E., and J. Lutkenhaus.** 1985. Overproduction of FtsZ induces minicell formation in *E. coli*. Cell **42**:941–949.
43. **Zagursky, R. J., and M. L. Berman.** 1984. Cloning vectors that yield high levels of single-stranded DNA for rapid DNA sequencing. Gene **27**:183–191.